Conf 930825 10

PNL-SA-22538

IRRADIATION PERFORMANCE OF 9-12 Cr FERRITIC/MARTENSITIC STAINLESS STEELS AND THEIR POTENTIAL FOR IN-CORE APPLICATION IN LWRs

R. H. Jones
D. S. Gelles

August 1993

Presented at the
Sixth International Symposium on
Environmental Degradation of Materials in
Nuclear Reactor Systems - Water Reactors
August 1-5, 1993
San Diego, CA

Work supported by
the U.S. Department of Energy
under Contract DE-AC06-76RLO 1830

Pacific Northwest Laboratory
Richland, Washington 99352

IRRADIATION PERFORMANCE OF 9-12 Cr FERRITIC/MARTENSITIC STAINLESS STEELS AND THEIR POTENTIAL FOR IN-CORE APPLICATION IN LWRs

R. H. Jones and D. S. Gelles
Pacific Northwest Laboratory
Richland, Washington 99352

Abstract

Ferritic-martensitic stainless steels exhibit radiation stability and stress corrosion resistance that make them attractive replacement materials for austenitic stainless steels for in-core applications. Recent radiation studies have demonstrated that 9% Cr ferritic/martensitic stainless steel had less than a 30°C shift in ductile-to-brittle transition temperature (DBTT) following irradiation at 365°C to a dose of 14 dpa. These steels also exhibit very low swelling rates, a result of the microstructural stability of these alloys during radiation. The 9 to 12% Cr alloys also exhibit excellent corrosion and stress corrosion resistance in out-of-core applications. Demonstration of the applicability of ferritic/martensitic stainless steels for in-core LWR application will require verification of the irradiation assisted stress corrosion cracking behavior, measurement of DBTT following irradiation at 288°C, and corrosion rate measurements for in-core water chemistry.

In-Core Experience of Ferritic/Martensitic Steels

Fast reactor experience

Application of ferritic/martensitic steels for use in intense radiation environments first evolved from fast breeder reactor experience. Initial experiments by Harkness et al. (1) gave the first demonstration that ferritic/martensitic steels provided enhanced swelling resistance, and based on that result, the ferritic/martensitic option, using the alloy HT-9, was included in the U.S. Department of Energy Cladding and Duct Materials Development Program (2). Similar motivations resulted in the inclusion of ferritic/martensitic steels (EM12, DIN 1.4914 and FV 448) in European fast reactor programs as well. In general, this meant that super 12% Cr steels intended for high temperature applications were studied, but it also included DT02 and DY005, 14% Cr dispersion strengthened ferritic steels.

The results of those efforts was the selection of ferritic/martensitic steels as the primary candidate alloy for fast breeder reactor applications (3,4), and inclusion of a ferritic/martensitic option for fusion reactor structural materials applications. Data bases for irradiation effects on properties have been established both for fast breeder (5) and fusion (6) applications. The major advantages of ferritic/martensitic steels in those applications are improved swelling and irradiation-creep resistance, as well as better thermal conductivity and improved thermal fatigue resistance and better corrosion resistance in liquid metals.

Light water experience

Ferritic/martensitic stainless steels have only been used in a few applications in LWRs and none of these include in-core use. These materials are widely used for steam turbine blading because of their strength and corrosion resistance while higher chromium ferritic stainless steels have been used in feedwater heaters. Type 405 and 409, both 12% Cr steels, are being used by U.S. manufacturers of recirculating steam generators because of the improved corrosion resistance of these steels relative to carbon steels. Also, Molander and

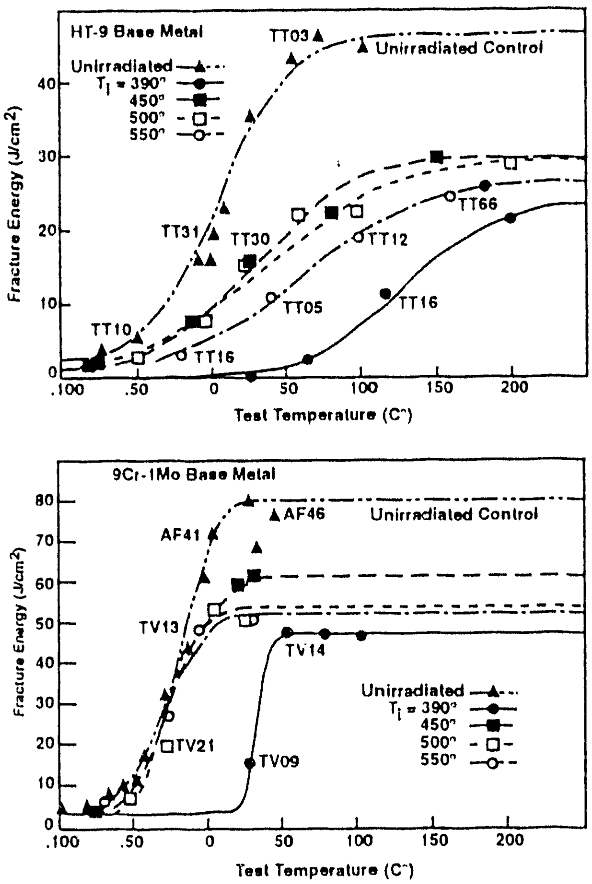

Figure 1: Charpy impact energy as a function of test temperature for specimens irradiated to 13 dpa in comparison to control conditions for a) HT-9 base metal and b) T9 base metal.

in T9. It is thought that the shift in DBTT is due to irradiation-induced hardening from dislocation and precipitate development (15). However, it has been argued that helium bubble development is in part responsible (16).

Alloy Development for Reduced Activation

As part of the fusion structural materials development effort, martensitic stainless steels have been designed to remove elements that produce long-lived radioactive isotopes (17). This has led to testing of tungsten stabilized martensitic steels that have shown great promise (18,19). Alloys with 7 to 9% Cr and 2% W have been found to give typical 12% Cr superalloy properties, but DBTT shifts following irradiation are negligible, whereas HT-9 develops shifts on the order of 120°C for similar irradiation conditions. Examples of DBTT

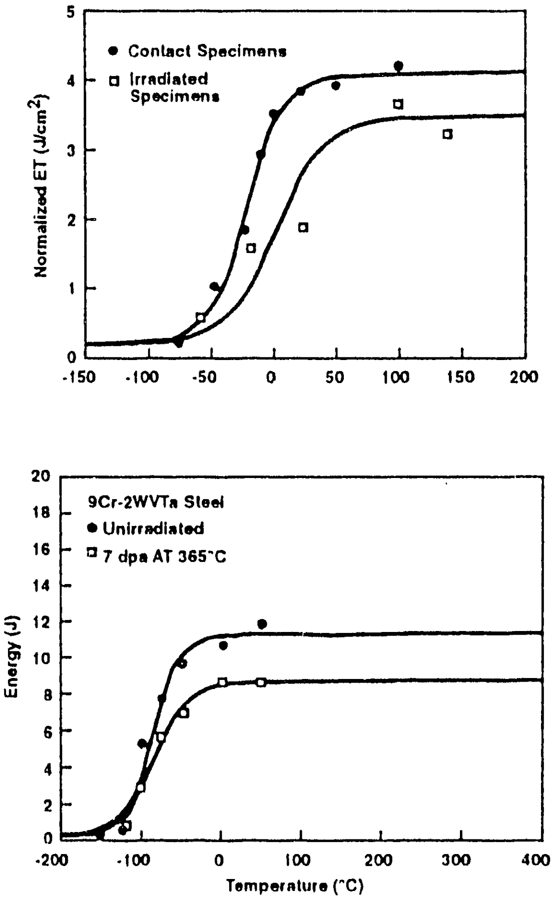

Figure 2. Charpy impact energy as a function of test temperature for specimens irradiated at 365°C to 10 dpa in comparison to control conditions for a) Fe-7Cr-2W and b) Fe-9Cr-2WVTa.

response in two tungsten stabilized steels are provided in Figure 2. This resistance to irradiation hardening arises from the fact that precipitation of α', nickel silicide and χ phases does not occur and tungsten additions tend to remain in solid solution (20). Further demonstration is provided in Figure 3 showing comparison of ultimate tensile strength and DBTT as a function of dose for the range of 5 to 9Cr reduced activation steels (21). Irradiation temperature is indicated for the tensile data whereas the DBTT data is based on irradiation at 370°C. Ultimate tensile strength increases only moderately following irradiation at 365 and 420°C, with softening found following irradiation at 485°C. Concurrently, DBTT shifts remain small.

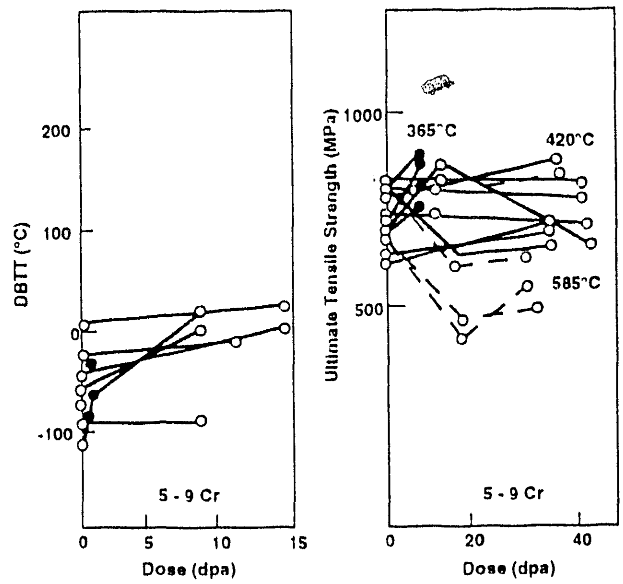

Figure 3. Ultimate tensile strength a) and DBTT b) for 7 to 9% Cr low activation alloys as a function of fast neutron dose.

<u>Stress corrosion behavior of ferritic/martensitic stainless steels</u>

Ferritic/martensitic stainless steels exhibit very good corrosion resistance in mildly corrosive environments. High chromium (> 18% Cr) ferritic stainless steels are often utilized for very corrosive environments. However, the corrosion resistance of Type 405 and 410 steels at 288°C in a solution of $NiCl_2$ (5800 ppm Cl^-) is a factor of 10 better than carbon steels. The corrosion rate of the 12% Cr steels is 100 mg/cm^2 after a 28 day exposure (22).

Hydrogen induced cracking is considered the most serious environmentally-induced cracking concern for 12% Cr steels. The crack growth rates of ferritic steels, including the 12% Cr versions, have been shown to be a function of the yield strength as shown in Figure 4. This dependence on yield strength is consistent with a hydrogen-induced cracking mechanism. The results shown in Figure 5 by Jones (23) also illustrate the dominant effect of cathodic potentials relative to anodic potentials on the strain to failure of a 12% Cr ferritic/martensitic steel. Cathodic hydrogen also produced considerably higher crack velocities than tests conducted in H_2O at 100°C. The results in Figure 6 show a stage II velocity of 3×10^{-6} mm/s at a very slightly cathodic potential for a steel with a yield strength of 500 MPa, but the crack velocity in 100°C H_2O, according to the data in Figure 4 should have been substantially less than 10^{-8} mm/s.

It has been demonstrated that hydrogen-induced crack growth is very temperature dependent. A schematic of the temperature dependence for hydrogen-induced cracking of ferritic steels is shown in Figure 7. The maximum crack velocity for ferritic steels occurs in the temperature range from 25 to about 100°C with a rapid decrease in crack velocity at temperatures above this range. Molander and Rosborg (7) found no evidence for stress corrosion cracking in Type 439 for tests conducted at 210°C in water with 1000 ppm Cl^- and 100 ppb O_2 and at a strain rate of 10^{-6}/s. Therefore, neither hydrogen-induced crack growth, which decreases rapidly above about 100°C, nor anodic dissolution type stress corrosion are expected to occur at 288°C.

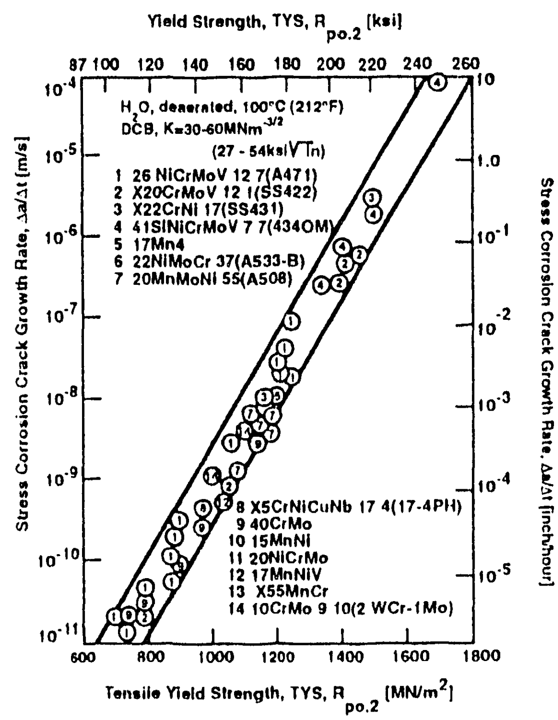

Figure 4. Crack velocity versus tensile yield strength for a variety of steels tested in water at 100°C including 12% Cr compositions.

Potential In-core LWR Applications for Ferritic/Martensitic Steels

The 9 to 12% Cr ferritic stainless, and in particular the 9% Cr steels, exhibit attractive radiation resistance in terms of

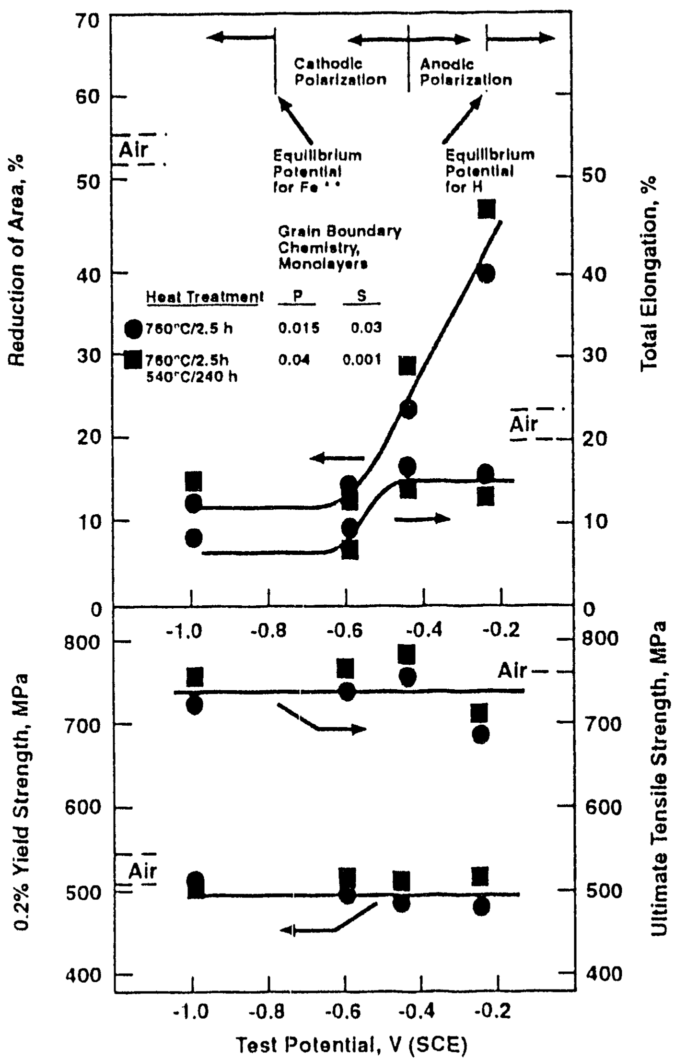

Figure 5. Straining electrode results for HT-9 tested in 1 N H_2SO_4 at 25°C.

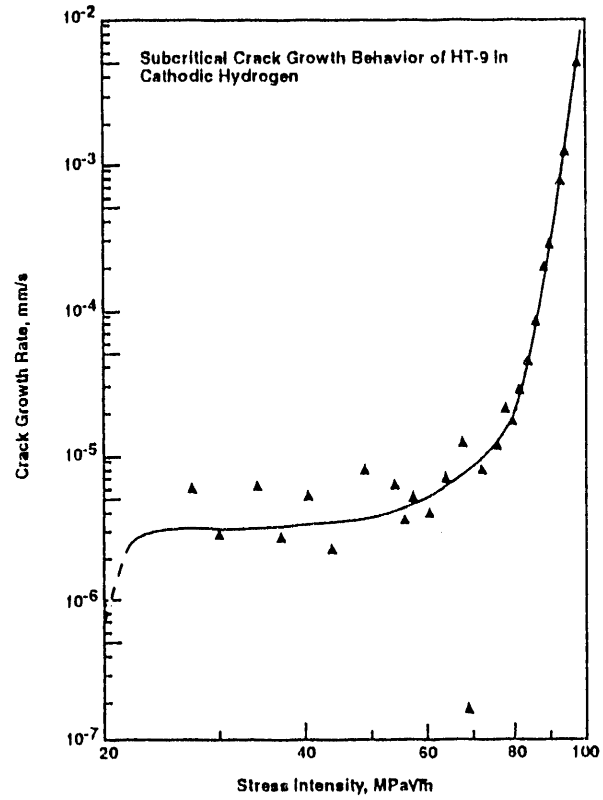

Figure 6. Crack growth rate versus stress intensity for HT-9 heat treated at 760°C for 2.5 h and tested in 1 N H_2SO_4 at 0.6 V (SCE).

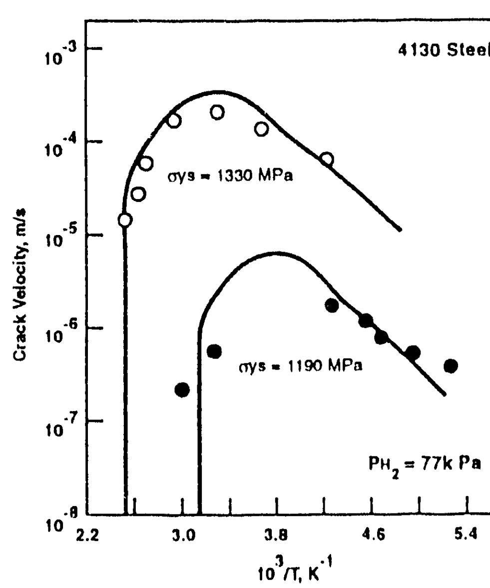

Figure 7. Crack velocity versus temperature for hydrogen induced crack growth of steel tested in hydrogen gas.

Rosborg (7) have evaluated the stress corrosion behavior of Type 409, 439 and 444 as alternate reheater tube materials and concluded that the Type 439 stainless steel was a suitable substitute. Syrett and Coit (8) noted that high-Cr ferritic stainless steel (AL29-4C) condenser tubes exhibited hydrogen-induced crack growth in a few instances. The cause was thought to be hydrogen generated by cathodic protection. However, no in-core experience exists on which to base a proposed use of ferritic/martensitic steels as replacement for austenitic stainless steels.

Radiation Response of Ferritic/Martensitic Steels

Swelling

A primary advantage of ferritic/martensitic steels for irradiation environments is high swelling resistance. This includes not only a high incubation fluence required for the onset of void swelling due to the complex tempered martensite microstructure, but also a very low steady state swelling rate (~0.05%/dpa). For example, HT-9 develops less than 1% void swelling following irradiation to 110 dpa at the peak swelling temperature of 420°C (9), and even for simple Fe-Cr binary alloys, swelling as measured by density change is less than 5% (10). As swelling and irradiation creep are coupled, irradiation-enhanced creep is also low (11).

Microstructure and microchemistry

Radiation damage in the peak swelling temperature regime results in observable microstructural development (12). The microstructural changes include dislocation, void and precipitate development. The dislocation development produces interstitial loops with both a/2<111> and a<100> Burgers vectors. With increasing dose, the loops grow and intersect, forming a complex dislocation network. However, the presence of tempered martensite subgrain boundaries discourages the formation of dislocation loops and network evolution. The excess vacancies that are created during dislocation evolution do recombine to form voids, and void swelling evolves concurrently. The reduced steady-state swelling rate in ferritic alloys is thought to be inherent in the crystal structure; the reduced packing density of first nearest neighbors in body-centered cubic structures (compared to face centered cubic structures) reduces the difference between the effective strain fields of vacancies and interstitials, and reduces the bias that promotes void swelling (13).

Concurrently, precipitate development often occurs, depending on alloy compositions. Most 12% Cr superalloys rely on $M_{23}C_6$ carbide stability for high temperature strength, but newer alloys also incorporate MC formation by additions of V and Nb. These precipitates remain stable under irradiation, but the MC composition is often found to change, taking up more Nb. However, irradiation-enhanced diffusion encourages the formation of Cr-rich α' when alloy compositions exceed 10% Cr. Additions of Ni and Si can form nickel silicide phases, and χ (chi) phase of two types (Fe,Cr,Mo and Fe,Cr,Mn) has been observed.

Many of the precipitate reactions are undoubtedly enhanced by radiation-induced solute segregation. For example, silicide formation is a consequence of interstitial drag of silicon to point defect sinks, such as voids and dislocations. Segregation has been shown to affect void shape and dislocation evolution (14). However, results have been contradictory with regard to chromium segregation. Some experiments have demonstrated chromium segregation to voids and grain boundaries, but others have failed to show such segregation. Therefore, it appears necessary to study a given material in the correct irradiation environment to demonstrate chromium segregation effects.

As deformation in body-centered cubic alloys is thermally activated at temperatures below about 0.3 Tm, a change in fracture mode can occur at low temperatures in ferritic/martensitic alloys, defined by the ductile-to-brittle transition temperature (DBTT). It has been generally found that irradiation causes an increase in the DBTT for ferritic/martensitic alloys. Figure 1 provides an example of DBTT behavior in HT-9, in comparison with an improved alloy denoted T9. The shift in DBTT is considerably smaller microstructural stability and DBTT. The improved microstructural stability relative to austenitic stainless steel suggests that these steels could be more resistant to irradiation assisted stress corrosion cracking (IASCC). However, further work is needed to verify the IASCC behavior of the ferritic/martensitic steels, the DBTT following irradiation at 288°C and the corrosion resistance of the 9% Cr steels.

Irradiation assisted stress corrosion

Irradiation-assisted stress corrosion cracking is a phenomenon that has been observed in austenitic stainless steels and nickel-based alloys following irradiation at around 300°C to a dose of about 1 dpa. This phenomenon is a concern for several in-core components in both BWRs and PWRs. It has been demonstrated (24) that this process requires an incubation irradiation period for non-sensitized material but not for sensitized material. It is believed that the incubation period is associated with a radiation damage process that requires an accumulated fluence of about 1 dpa.

Several radiation damage processes have been considered as the cause of IASCC: 1) radiation-induced segregation of impurities to grain boundaries, 2) radiation-induced depletion of Cr from the grain boundaries and 3) radiation-induced hardness increases. Radiation-induced segregation of elements to internal and external surfaces has been the subject of extensive study by Okamoto et al. (25). Jones (26) also found considerable P surface segregation in ion irradiated Type 316 SS and Ni. Radiation-induced depletion of Cr from interfaces occurs by an inverse Kirkendall effect. Ion-irradiation results by Bruemmer et al. (27) have confirmed that radiation-induced Cr depletion occurs and that it can be predicted by the inverse Kirkendall effect. Radiation hardening and its effect on grain boundary creep/sliding is also being considered as a possible explanation by Bruemmer et al. (27).

Although the specific mechanisms of IASCC are unconfirmed and could be a combination of several processes, it can be demonstrated that ferritic/martensitic steels are likely to be less susceptible to IASCC than are austenitic alloys. For instance, Jones (26) found very little surface segregation in ion irradiated HT-9 and FE+01% P alloys in the same study that found significant P segregation in Type 316 SS and Ni. Kimura et al. (28) found a moderate increase in the grain boundary Si and a small increase in the grain boundary P concentration in a 9% Cr-1%W-2%Mn steel irradiated at 365°C to 10 dpa. Whether similar levels of segregation will occur in Mn free steels or whether the 0.15 monolayers of Si and 0.04 monolayers of P observed by Kimura et al . (28) will affect stress corrosion is not known. Jones (23) found little effect of similar grain boundary concentrations of P on the stress corrosion cracking of a 12% Cr steel at either anodic or cathodic potentials.

Chromium depletion by the inverse Kirkendall effect occurs because of an excess vacancy flux to grain boundaries. The low swelling and microstructural stability of irradiated 9 to 12% Cr steels suggests that large microchemical gradients do not occur in these materials. Low swelling in ferritic alloys has been previously associated with the bcc crystal structure, but recent studies of binary bcc alloys indicate that this low swelling is not inherent in the crystal structure, but may be the result of impurities. In any event, the combination of impurities and complex microstructure of ferritic/martensitic steels results in a very radiation resistant material. This radiation resistance is also demonstrated by the small increase in hardness shown in Figure 3 for material irradiated at 365 to 585°C.

Therefore, impurity segregation, Cr depletion and hardness increase, which are considered primary factors in the cause of IASCC in austenitic alloys, occur to a much lesser degree in 9 to 12% Cr steels. This radiation stability could lead to greatly improved in-core performance for the 9 to 12% Cr steels relative to austenitic stainless steels.

Issues in the in-core application of 9 to 12% Cr steels

Several questions must be resolved regarding the application of these steels for in-core service. These issues include: 1) demonstration of IASCC performance, 2) DBTT shift for lower irradiation temperatures, (3) corrosion rates and radioactive material transfer for in-core conditions and 4) relative fabrication, etc costs. Issue number 1 has been discussed above, but it will be necessary to demonstrate that the potential for improved resistance to IASCC is indeed realized in these steels. As shown in Figure 3 the DBTT of the 5 to 9% Cr steels following irradiation at 365°C to 13 dpa is around 0°C. A DBTT of 0°C is certainly adequate for in-core service; however, it will be necessary that irradiation at 288°C does not induce greater hardness increases and hence greater shifts in DBTT. Since the DBTT in these steels is still suitable at 13 dpa and 365°C, it likely will be suitable at 1-5 dpa and 288°C. The 9 to 12% Cr steels exhibit very good corrosion behavior even in high Cl⁻ concentrations. However, even small differences in corrosion rate can result in large differences in radioactive isotope transport and therefore in the background radiation levels within the plant. Quantitative corrosion rate comparisons between 18% Cr-8% Ni austenitic stainless steels and the 9 to 12% Cr ferritic/martensitic steels will be necessary to address this issue.

Summary

Ferritic/martensitic stainless steels exhibit radiation damage characteristics which suggest that their in-core performance in LWRs could be very good. The excellent radiation resistance as evidenced by low swelling and microstructural stability indicate that these steels may also be resistant to IASCC. Observations of low radiation-induced impurity segregation are consistent with this conclusion. Small increases in hardness and DBTT at fluences of up to 13 dpa following irradiation at 365°C also illustrate the radiation resistance of these steels. The radiation effects data available for these steels clearly suggests their in-core performance could exceed that of austenitic stainless steels. One area of concern is the corrosion rate and hence the radioactive isotope transfer and radiation background levels in the plant.

Acknowledgments

The authors wish to acknowledge the support for this research from the Office of Basic Energy Sciences and the Office of Fusion Energy of the U.S. Department of Energy under contract DE-AC06-76RLO 1830.

References

1. S. D. Harkness, B. J. Kestel and P. Okamoto, in: Radiation Induced Voids in Metals, CONF-710601, (1972) p. 334.

2. J. J. Laidler, J. J. Holmes, and J. W. Bennett, U.S. Programs on Reference and Advanced Cladding/Duct Materials, in: Radiation Effect in Breeder Reactor Structural Materials, M. L. Bleiberg and J. W. Bennett, Eds. AIME, New York, NY (1977), pp. 41-63. See Session I for descriptions of other European programs.

3. D. S. Gelles, Optimization of Martensitic Stainless Steels for Nuclear Reactor Application, in Optimizing Materials for Nuclear Applications, F. A. Garner, D. S. Gelles and F. W. Wiffen, Ed., TMS, Warrendale, PA (1985), pp. 63-71.

4. D. S. Gelles, Research and Development of Iron-based Alloys for Nuclear Technology, ISIJ International, 30 (1990), pp. 905-916.

5. J. L. Straalsund and D. S. Gelles, presented at the Topical Conference on Ferritic Alloys for Use in Nuclear Energy Technologies, Snowbird, UT, HEDL-SA-2771, May 1983.

6. D. S. Gelles, J. Nucl. Mater., 194 (1987), p. 192.

7. A Molander and B. Rosborg, Stress Corrosion Cracking Resistance of Alternative Reheater Tube Materials, in: Proceedings of the International Symposium on Environmental Degradation of Materials in Nuclear Power Systems-Water Reactors, Myrtle Beach, South Carolina, Aug 22-25, 1983, National Association of Corrosion Engineers, 1440 S. Creek Dr., Houston, TX 77084.

8. B. Syrett and R. Coit, ibid, p. 87.

9. D. S. Gelles and A. Kohyama, Microstructural Examination of HT-9 Irradiated in the FFTF/MOTA to 110 DPA, Fusion Reactor Materials for the period ending March 31, 1989, DOE/ER-0313/6, pp. 193-199.

10. D. S. Gelles and R. L. Meinecke (Ermi), Alloy Development for Irradiation Performance Semiannual Progress Report for the Period Ending September 30, 1983, DOE/ER-0045/11, p. 103.

11. R. J. Puigh and D. S. Gelles, Irradiation Creep of Ferritic (and Other BCC) Alloys, Fusion Reactor Materials for the period ending March 31, 1989, DOE/ER-0313/6, pp. 201-224.

12. D. S. Gelles and L. E. Thomas, in: Proceedings of Topical Conference on Ferritic Alloys for Use in Nuclear Energy Technologies, J. W. Davis and D. J. Michel, Eds., AIME, Warrendale, PA 1984, pp. 559-568.

13. J. J. Sniegowski and W. G. Wolfer, IBID, pp. 579-586.

14. D. S. Gelles, Effects of Radiation on Materials Vol. I, ASTM 1046, ASTM, Philadelphia, PA (1990), pp. 73-97.

15. W. L. Hu and D. S. Gelles, Charpy Impact Test Results of Ferritic Alloys Irradiated to 10 dpa, in Effects of Radiation on Materials: 14th International Symposium, Volume 2, ASTM STP 1046, N. H. Packanm, R. E. Stoller and A. S. Kumar, Eds., American Society for Testing and Materials, Philadelphia (1990), pp. 453-458.

16. R. L. Klueh and D. J. Alexander, J. Nucl. Mater., 179-181 (1991), pp. 733-736.

17. R. L. Klueh, D. S. Gelles, S. Okada and N. Packan, Eds., Reduced Activation Materials for Fusion Reactors, ASTM STP 1047, ASTM, Philadelphia, PA (1990).

18. N. S. Cannon and D. S. Gelles, J. Nucl. Mater., 186 (1991), pp. 68-76.

19. R. L. Klueh and D. J. Alexander, in Fusion Reactor Materials Semiannual Progress report for the period Ending September 30, 1990, DOE/ER-0313/9, pp. 106-112.

20. D. S. Gelles in: Reduced Activation Materials for Fusion Reactors, R. L. Klueh, D. S. Gelles, A. Okada and N. Packan, Eds., ASTM STP 1047, ASTM, Philadelphia, PA (1990), pp. 113-129.

21. D. S. Gelles, Fusion Reactor Materials Semiannual Progress Report for the Period Ending September 30, 1992, DOE/ER0313/13, p. 157.

22. R. A. Vaia, G. Economy, M. J. Wootten and R. G. Aspden, Denting of Steam Generator Tubes in PWR Plants, Mater. Perform. Vol 19, Feb 1980, p. 9

23. R. H. Jones, Hydrogen-Induced Subcritical Crack Growth of a 12Cr-1Mo Ferritic Stainless Steel, Metall. Trans. A, Vol 17A (1986) p. 1229.

24. P. L. Andresen, Irradiation-Assisted Stress Corrosion Cracking, in: Stress-Corrosion Cracking: Materials Performance and Evaluation, R. H. Jones, Ed., (1992), ASM Int., Materials Park, OH, p. 181.

25. P. R. Okamoto and H. Wiedersich, Segregation of Alloying Elements to Free Surfaces During Irradiation, J. Nucl. Mater., 53 (1974) p. 336.

26. R. H. Jones, Some Radiation Damage-Stress Corrosion Synergisms in Austenitic Stainless Steel, in: Proceedings of the Second International Symposium on Environmental Degradation of Materials in Nuclear Power Systems-Water Reactors, Monterey, CA, Sept. 1985, American Nuclear Society, LaGrange Park, Ill 60525, (1986), p. 173.

27. S. M. Bruemmer and E. P. Simonen, Radiation Hardening and Radiation-Induced Chromium Depletion Effects on Itergranular Stress Corrosion Cracking of Austenitic Stainless Steel, Corrosion/93, paper #616.

28. A. Kimura, L. A. Charlot, D. S. Gelles, D. R. Baer and R. H. Jones, Irradiation Induced Changes in the Grain Boundary Chemistry of High-Manganese Low Activation Martensitic Steels, J. of Nuclear Materials, 191-194 (1992) p. 885.

END

DATE FILMED

12/23/93